Superstructure-Dependent Loading of DNA Origami Nanostructures with a Groove-Binding Drug

Fabian Kollmann,[†] Saminathan Ramakrishnan,[†] Boxuan Shen,[‡] Guido Grundmeier,[†] Mauri A. Kostiainen,[‡] Veikko Linko[,†,‡] and Adrian Keller*[,†]*

† Technical and Macromolecular Chemistry, Paderborn University, Warburger Str. 100, 33098 Paderborn, Germany.

‡ Biohybrid Materials, Department of Bioproducts and Biosystems, Aalto University, P. O. Box 16100, FI-00076 Aalto, Finland.

Individual UV/Vis absorbance spectra of MB-DNA binding in water and buffer

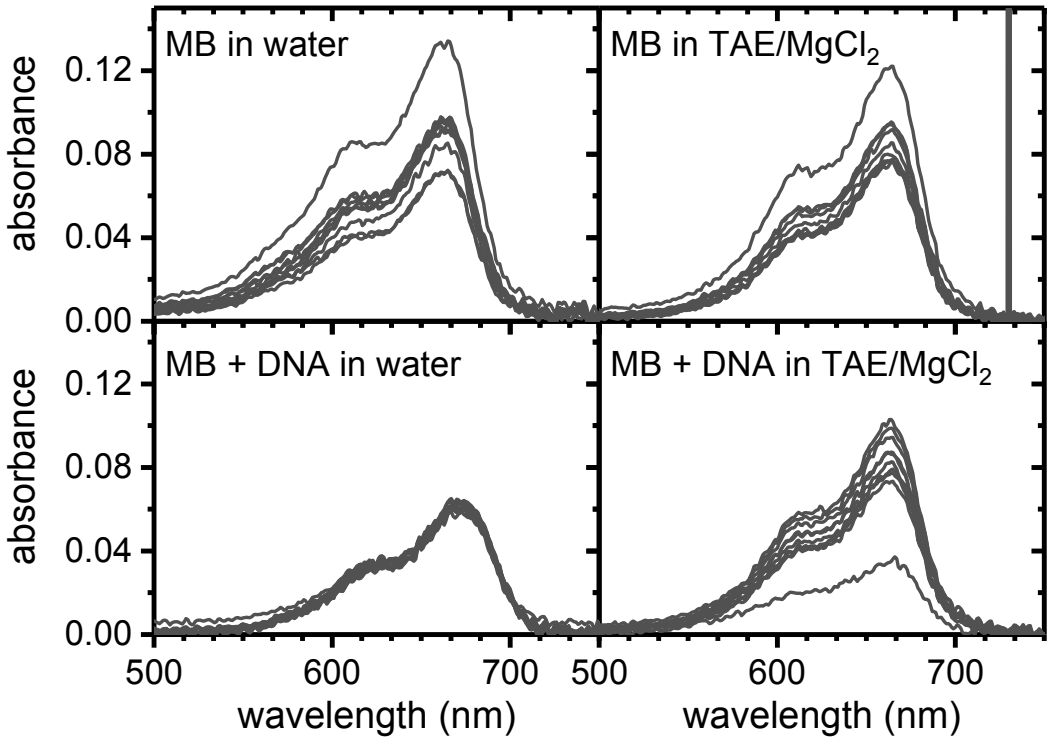

Figure S1. *Individual UV/Vis absorbance spectra of 20 µM MB with and without genomic dsDNA from salmon testes in water and $MgCl_2$-containing TAE buffer (see Figure 1a in the main article).*

Paired and unpaired bases in the different DNA origami designs

Table S1: *Numbers of base pairs and unpaired nucleotides from scaffold, staples, and overhangs of the DNA origami investigated in this work.*

DNA origami	base pairs	unpaired nucleotides
6HB	7,140	109
60HB	5,460	1,789
Z shape	6,942	1,155
triangle	7,196	51
bow tie	6,962	1,167

Netropsin competition assay for the different DNA origami nanostructures

The netropsin competition assay shown in Figure 1b of the main article has been repeated for all the DNA origami nanostructures investigated in this work. The results are shown in Figure S2. For all DNA origami nanostructures, an increase in absorption upon addition of large amounts of netropsin is observed, albeit to different extents. These differences may reflect different dependencies of netropsin and MB binding on minor groove dimensions.

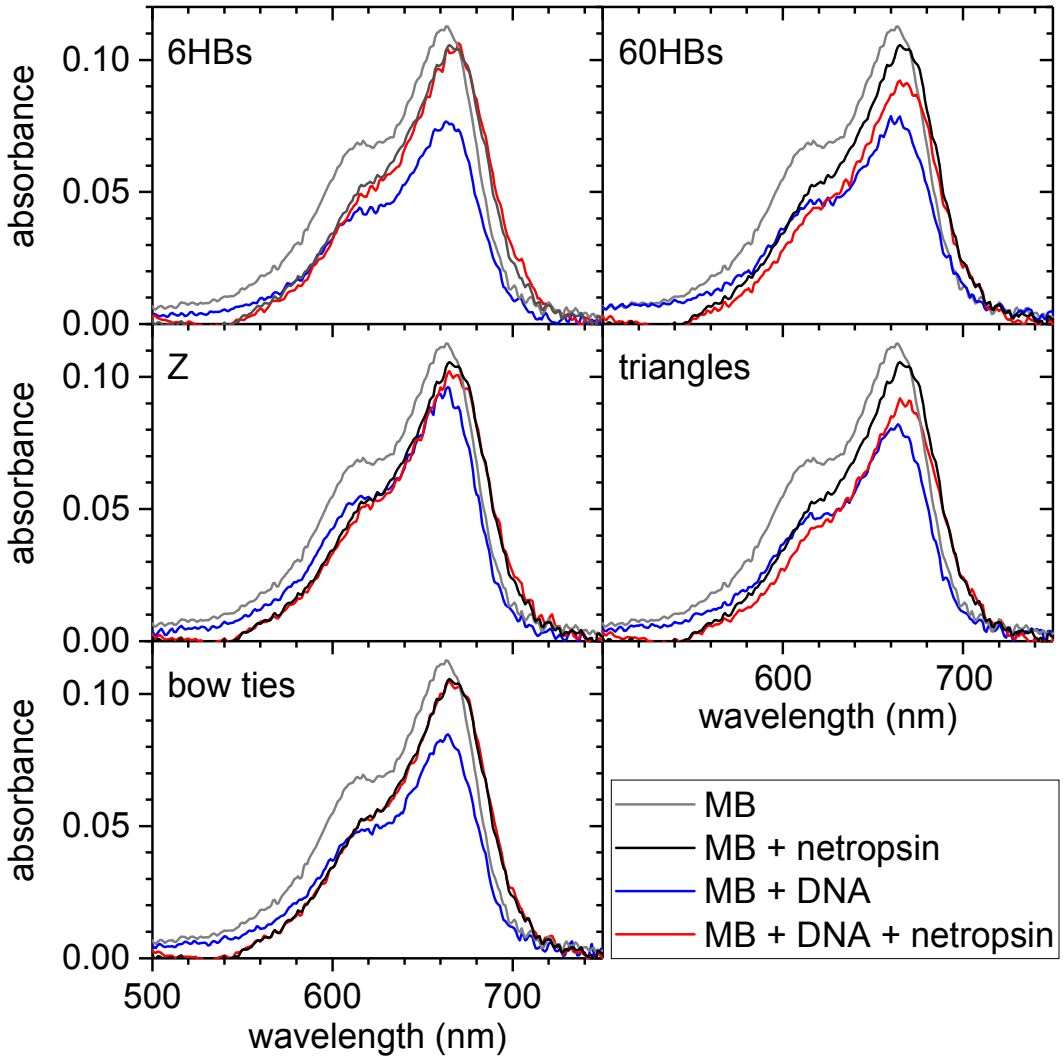

Figure S2. *UV-Vis spectra of the competition between 20 μM MB and 500 μM netropsin for minor groove binding to the different DNA origami nanostructures in 1x TAE buffer supplemented with 10 mM $MgCl_2$. DNA origami concentrations were 7.3 nM (6HBs and 60HBs), 5.3 nM (Z shapes and bow ties), and 5.5 nM (triangles), respectively.*

Additional independent concentration series and binding isotherms

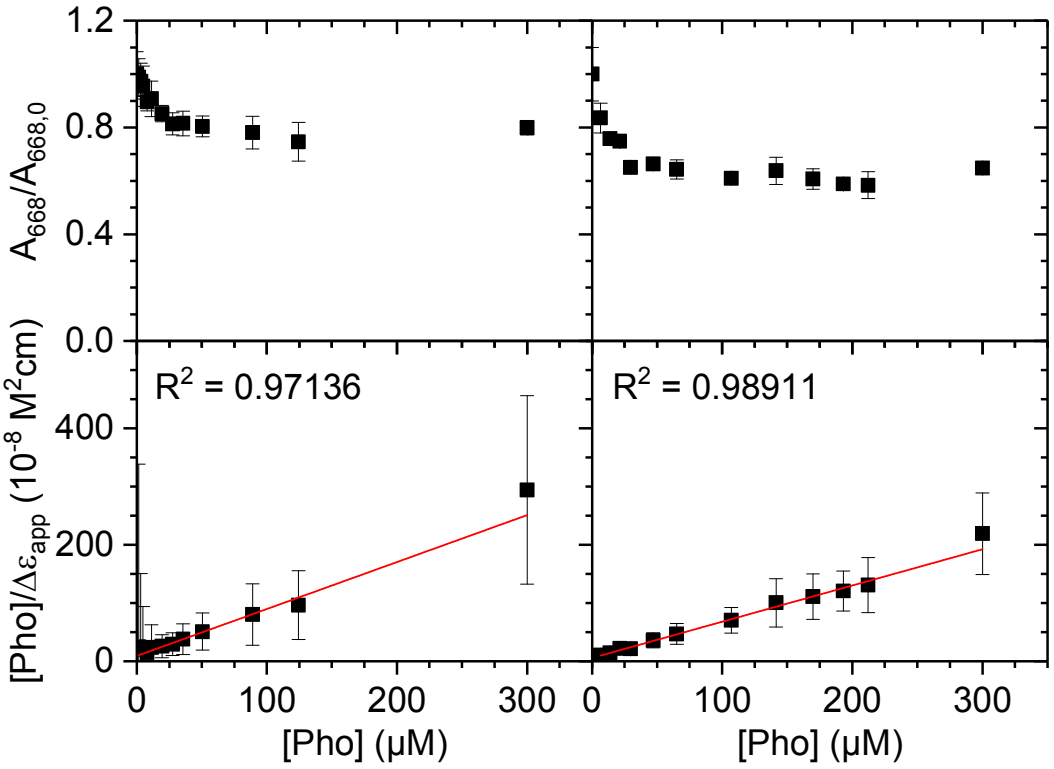

Figure S3. *Additional independent concentration series and binding isotherms for dsDNA.*

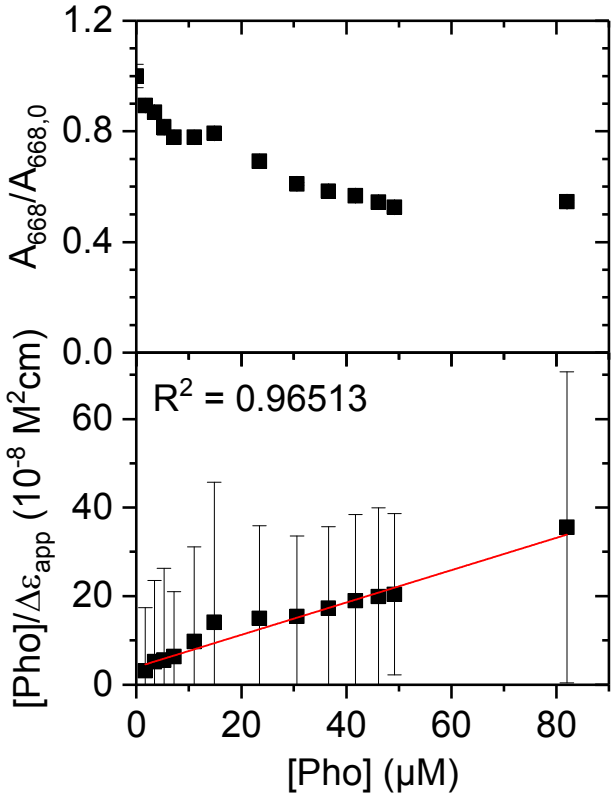

Figure S4. *Additional independent concentration series and binding isotherm for 6HBs.*

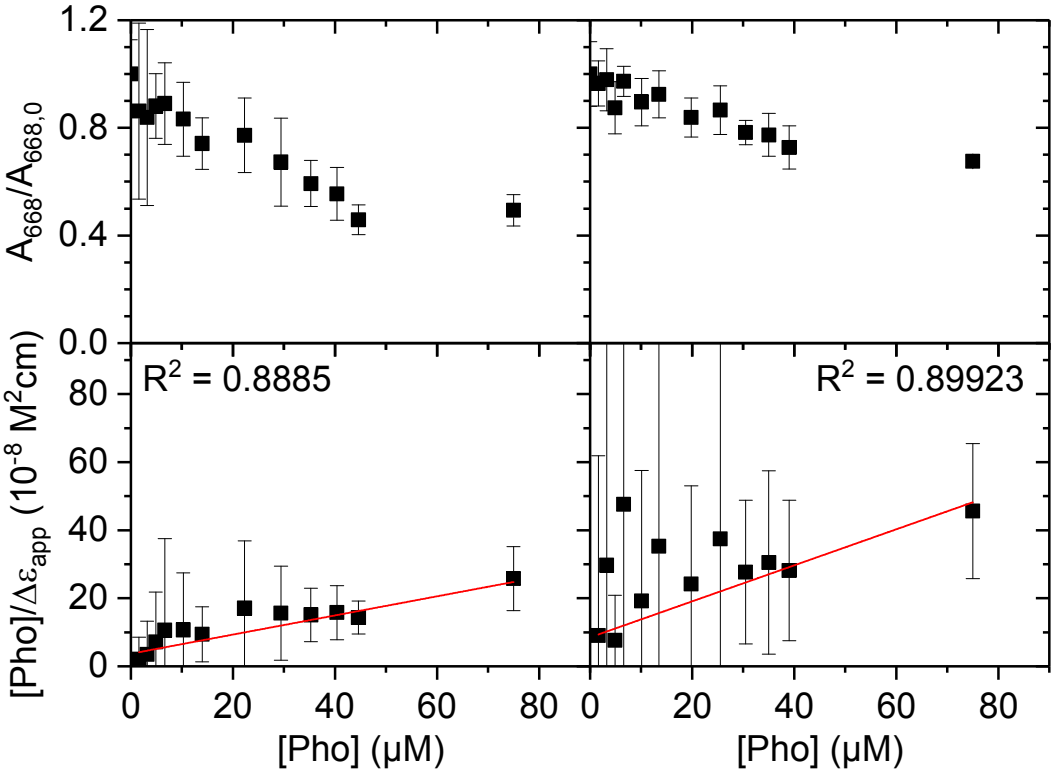

Figure S5. *Additional independent concentration series and binding isotherms for 60HBs.*

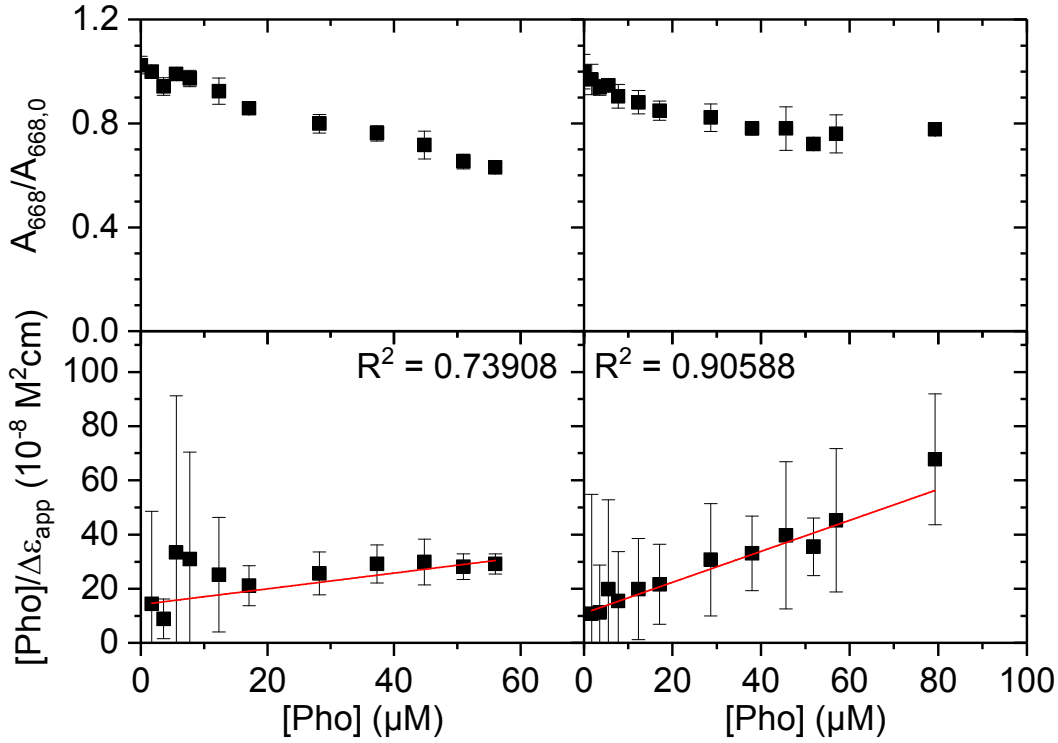

Figure S6. *Additional independent concentration series and binding isotherms for Z shapes.*

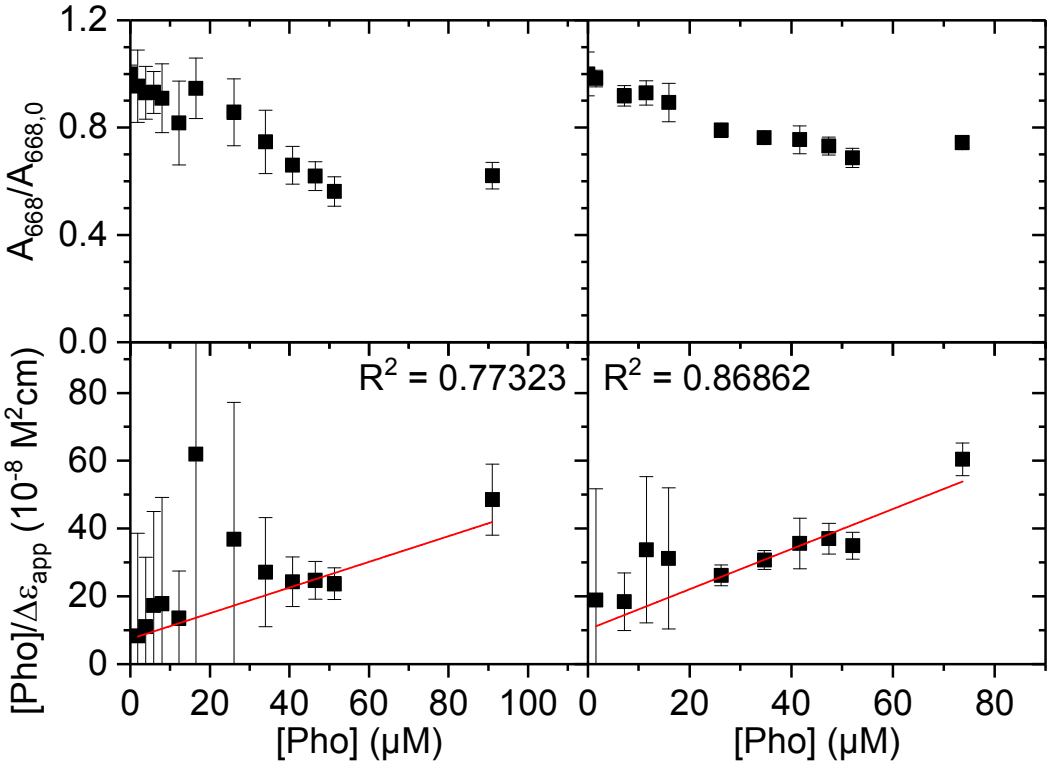

Figure S7. *Additional independent concentration series and binding isotherms for triangles.*

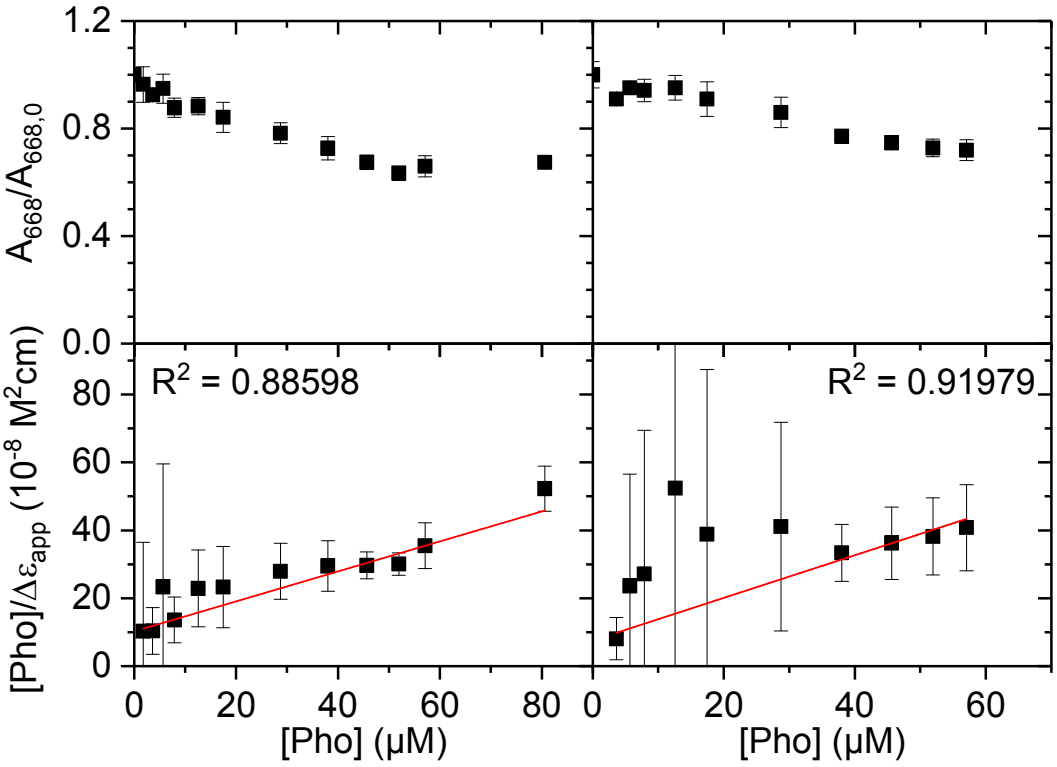

Figure S8. *Additional independent concentration series and binding isotherms for bow ties.*

MB loading efficiency

Table S2: *Average DNA origami concentrations at which saturation of the MB absorbance was observed and corresponding numbers of bound MB molecules per DNA origami.*

DNA origami	saturation concentration (nM)	# MB per DNA origami
6HB	2.9 ± 0.5	6,897 ± 1,160
60HB	3.5 ± 0.6	5,714 ± 951
Z shape	2.9 ± 0.5	6,897 ± 1,151
triangle	3.0 ± 0.2	6,667 ± 479
bow tie	2.7 ± 0.3	7,407 ± 812

Averaging of K_d values

Table S3: *Individual K_d values (in µM) of each DNA structure obtained in the independent concentration series and the resulting averaged K_d values (highlighted). The errors of the individual K_d values have been calculated from the errors of the fits (see Figs. S3 – S8) using full propagation of error. The averaged K_d values are listed with the standard errors of the mean as errors.*

dsDNA	6HB	60HB	Z	triangle	bow tie
11.4 ± 2.7	10.9 ± 2.3	13.0 ± 5.6	23.8 ± 7.3	19.6 ± 11.9	11.0 ± 3.0
9.9 ± 1.9	11.5 ± 3.3	16.1 ± 5.6	48.7 ± 18.5	17.3 ± 8.2	12.0 ± 4.9
10.2 ± 1.6		15.1 ± 3.3	19.1 ± 5.9	15.0 ± 5.4	23.2 ± 8.0
10.2 ± 1.2	11.2 ± 2.0	14.6 ± 3.0	26.1 ± 5.0	17.1 ± 4.7	15.4 ± 3.2